Background Modeling and Statistical Inference for WIMP Searches in XENON1T

E. Aprile,[1] J. Aalbers,[2] F. Agostini,[3] M. Alfonsi,[4] L. Althueser,[5] F. D. Amaro,[6] M. Anthony,[1] F. Arneodo,[7] L. Baudis,[8] B. Bauermeister,[9] M. L. Benabderrahmane,[7] T. Berger,[10] P. A. Breur,[2] A. Brown,[2] A. Brown,[8] E. Brown,[10] S. Bruenner,[11] G. Bruno,[7] R. Budnik,[12] C. Capelli,[8] J. M. R. Cardoso,[6] D. Cichon,[11] D. Coderre,[13] A. P. Colijn,[2] J. Conrad,[9] J. P. Cussonneau,[14] M. P. Decowski,[2] P. de Perio,[1] P. Di Gangi,[3] A. Di Giovanni,[7] S. Diglio,[14] A. Elykov,[13] G. Eurin,[11] J. Fei,[15] A. D. Ferella,[9] A. Fieguth,[5] W. Fulgione,[16,17] A. Gallo Rosso,[16] M. Galloway,[8] F. Gao,[1] M. Garbini,[3] C. Geis,[4] L. Grandi,[18] Z. Greene,[1] H. Qiu,[12] C. Hasterok,[11] E. Hogenbirk,[2] J. Howlett,[1] R. Itay,[12] F. Joerg,[11] B. Kaminsky,[13,*] S. Kazama,[8,†] A. Kish,[8] G. Koltman,[12] H. Landsman,[12] R. F. Lang,[19] L. Levinson,[12] Q. Lin,[1] S. Lindemann,[13] M. Lindner,[11] F. Lombardi,[15] J. A. M. Lopes,[6,‡] J. Mahlstedt,[9] A. Manfredini,[12] T. Marrodán Undagoitia,[11] J. Masbou,[14] D. Masson,[19] M. Messina,[7] K. Micheneau,[14] K. Miller,[18] A. Molinario,[16] K. Morå,[9] M. Murra,[5] J. Naganoma,[20] K. Ni,[15] U. Oberlack,[4] B. Pelssers,[9] F. Piastra,[8] J. Pienaar,[18] V. Pizzella,[11] G. Plante,[1] R. Podviianiuk,[16] N. Priel,[12] D. Ramírez García,[13] L. Rauch,[11] S. Reichard,[8] C. Reuter,[19] B. Riedel,[18] A. Rizzo,[1] A. Rocchetti,[13] N. Rupp,[11] J. M. F. dos Santos,[6] G. Sartorelli,[3] M. Scheibelhut,[4] S. Schindler,[4] J. Schreiner,[11] D. Schulte,[5] M. Schumann,[13] L. Scotto Lavina,[21] M. Selvi,[3] P. Shagin,[20] E. Shockley,[18] M. Silva,[6] H. Simgen,[11] D. Thers,[14] F. Toschi,[3,13] G. Trinchero,[17] C. Tunnell,[18] N. Upole,[18] M. Vargas,[5] O. Wack,[11] H. Wang,[22] Z. Wang,[16] Y. Wei,[15] C. Weinheimer,[5] C. Wittweg,[5] J. Wulf,[8] J. Ye,[15] Y. Zhang,[1] and T. Zhu[1]

(XENON Collaboration),[§]

[1]*Physics Department, Columbia University, New York, NY 10027, USA*
[2]*Nikhef and the University of Amsterdam, Science Park, 1098XG Amsterdam, Netherlands*
[3]*Department of Physics and Astronomy, University of Bologna and INFN-Bologna, 40126 Bologna, Italy*
[4]*Institut für Physik & Exzellenzcluster PRISMA, Johannes Gutenberg-Universität Mainz, 55099 Mainz, Germany*
[5]*Institut für Kernphysik, Westfälische Wilhelms-Universität Münster, 48149 Münster, Germany*
[6]*LIBPhys, Department of Physics, University of Coimbra, 3004-516 Coimbra, Portugal*
[7]*New York University Abu Dhabi, Abu Dhabi, United Arab Emirates*
[8]*Physik-Institut, University of Zurich, 8057 Zurich, Switzerland*
[9]*Oskar Klein Centre, Department of Physics, Stockholm University, AlbaNova, Stockholm SE-10691, Sweden*
[10]*Department of Physics, Applied Physics and Astronomy, Rensselaer Polytechnic Institute, Troy, NY 12180, USA*
[11]*Max-Planck-Institut für Kernphysik, 69117 Heidelberg, Germany*
[12]*Department of Particle Physics and Astrophysics, Weizmann Institute of Science, Rehovot 7610001, Israel*
[13]*Physikalisches Institut, Universität Freiburg, 79104 Freiburg, Germany*
[14]*SUBATECH, IMT Atlantique, CNRS/IN2P3, Université de Nantes, Nantes 44307, France*
[15]*Department of Physics, University of California, San Diego, CA 92093, USA*
[16]*INFN-Laboratori Nazionali del Gran Sasso and Gran Sasso Science Institute, 67100 L'Aquila, Italy*
[17]*INFN-Torino and Osservatorio Astrofisico di Torino, 10125 Torino, Italy*
[18]*Department of Physics & Kavli Institute for Cosmological Physics, University of Chicago, Chicago, IL 60637, USA*
[19]*Department of Physics and Astronomy, Purdue University, West Lafayette, IN 47907, USA*
[20]*Department of Physics and Astronomy, Rice University, Houston, TX 77005, USA*
[21]*LPNHE, Université Pierre et Marie Curie, Université Paris Diderot, CNRS/IN2P3, Paris 75252, France*
[22]*Physics & Astronomy Department, University of California, Los Angeles, CA 90095, USA*

(Dated: August 17, 2018)

PACS numbers: 95.35.+d, 14.80.Ly, 29.40.-n, 95.55.Vj
Keywords: Dark Matter, Direct Detection, Xenon, Data Analysis

I. INTRODUCTION

II. DETECTOR SIGNAL RESPONSE MODEL

XENON1T WIMP signal and background model used in the statistical inference are built based on the simulation which takes into consideration the detailed characterizations of the detector systematics, as well as the most comprehensible modeling of the recombination process of the liquid xenon. The coherent modeling of the electronic recoils (ERs) and nuclear recoils (NR) is of high accuracy

*Also at Albert Einstein Center for Fundamental Physics, University of Bern, Bern, Switzerland
†Also at Kobayashi-Maskawa Institute, Nagoya University, Nagoya, Japan
‡Also at Coimbra Polytechnic - ISEC, Coimbra, Portugal
§xenon@lngs.infn.it

in terms of the uncertainty of the nuisance parameters and their correlations. In this chapter, the details of the detector signal response model will be given.

A. Basic Signal Response in Liquid Xenon

B. Recombination in Low Energy

C. Influence by Detector Reconstruction

III. BACKGROUND AND DARK MATTER SIGNAL MODEL

A. Electronic Recoil Backgrounds

B. Nuclear Recoil Backgrounds

1. Radiogenic Neutrons

2. Solar Neutrino

C. Surface Backgrounds

Just add the content to start, will modify the description further.....

Interactions in the inner part of the detector can be nicely modelled by combining our knowledge on LXe's properties to ionizing particles and the detector related properties like charge/light collections. In cases where the latter information is missing/incomplete, we need to develop new algorithms to model the events. In this and following sections, two classes of background components are analyzed for the XENON1T dark matter searches.

As has been proved by several experiments [**? ?**], detector surfaces exposed long to ambient air during construction phase are contaminated by large amount of radon progeny, in particular the ^{210}Pb. With a 22 y half-life, ^{210}Pb basically decays constantly within the XENON1T's operation of a few years. For dark matter searches, ion recoil of ^{206}Pb from ^{210}Po α-decays, β-decays and the resulting X-rays, Auger electrons of ^{210}Pb are particularly important. Due to unknown LXe's properties and detector physics in presence of PTFE as well as the complicated decay structures, a precise modeling based on Monte-Carlo simulation approach has not been achieved in XENON1T yet. Instead, a data driven approach is adopted to predict the event distribution of this background.

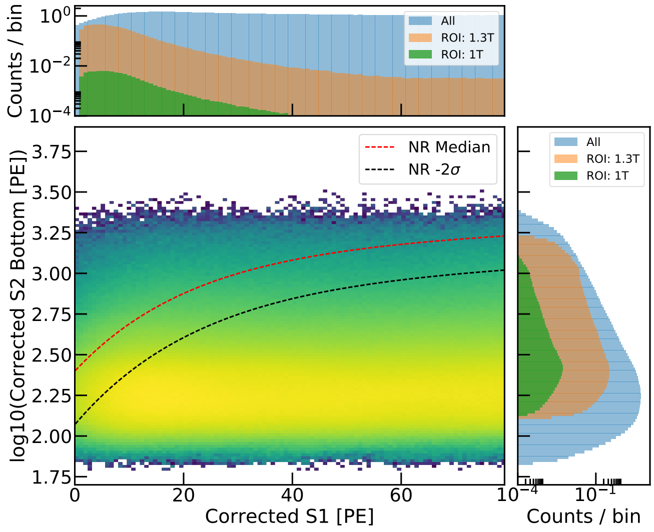

FIG. 1:

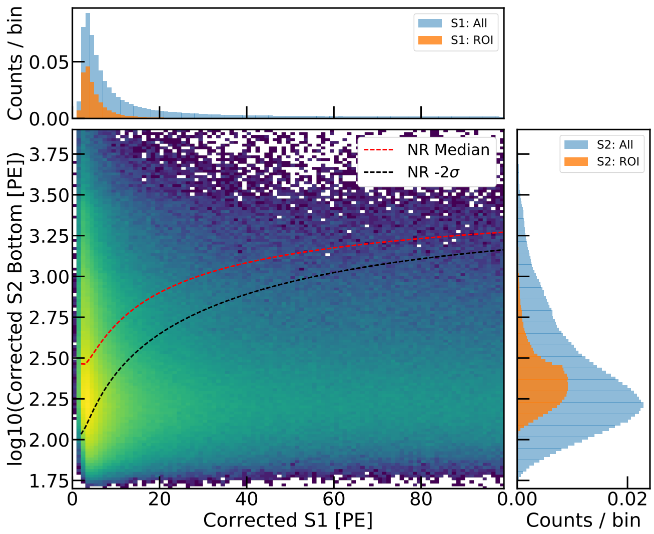

FIG. 2:

D. Accidental Pile-up

E. Dark Matter Signal Model

IV. STATISTICAL INFERENCE

A. General Statistical Method

B. Inference of XENON1T Data

C. The XENON1T Combined Likelihood

The log-likelihood used in the spin-independent analysis is a sum of extended un-binned likelihoods for the two science runs, extended un-binned likelihoods for ER

calibration data, and terms expressing ancillary measurements of nuisance parameters θ_m:
Where SR runs over data-taking periods, SR0 and SR1, σ is the WIMP-nucleon cross-section, and $\log\mathcal{L}_{\rm sci}$,$\log\mathcal{L}_{\rm cal}$ are the likelihood terms for the dark matter search data and ^{220}Rn calibration data, respectively. Ancillary measurements The un-binned likelihoods take the form:

D. Analysis Dimensions

E. Core Volume Segmentation

F. Safeguard

A mismodelling term, proposed in [43] is added to the ER model, consisting of a signal-like component added or subtracted to the nominal ER model:
Since the PDF is constrained to be non-negative, the

G. Nuisance Parameters

H. Trial Correction

As discovery significances are computed for WIMP-masses between 6 and 1000 GeV, the final p-value of the experiment must reflect that multiple hypotheses were tested, and the lowest local p-value is picked as the most significant excess. The result is correlated between multiple masses, with a lower correlation between the peaked low-mass WIMP, and complete correlation between dark matter masses above 200 GeV, where the recoil spectrum converges. Toy Monte-Carlo data samples are generated without a dark matter signal, and discovery significances are computed for the entire mass range. The lowest local p-value is stored to compute the distribution of most significant local p-values. The global significance of the actual dataset is the percentile of the lowest p-value from the actual data of this distribution. Using local p-values rather than log-likelihood rations directly corrects for the uneven weighting that would result as different masses do not have the same null-distribution of the discovery log-likelihood ratio.

I. Coverage

The fraction of repeated experiments where the confidence interval contains the true parameter is called the coverage. Perfect coverage is equal to the confidence interval, 0.9 in the case of XENON. As the experiment decided to report only the upper edge of the confidence interval for discovery significances $< 3\sigma$, there will be over-coverage at very low signal sizes. This has a similar effect to the power constraint. Figure 3n shows the

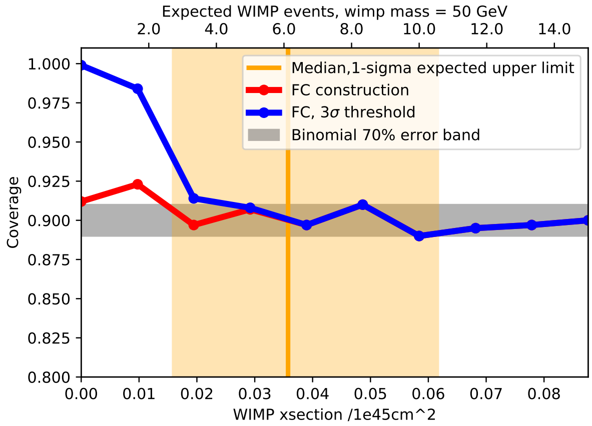

FIG. 3:

coverage for a 50 GeV WIMP, with the red line representing the profile construction coverage, and blue the coverage including the 3σ threshold. The orange band, shows the $-\sigma$ to σ sensitivity band. The result is consistent with perfect coverage (marked by the gray band, including limited statistics), with overcoverage for the 3σ threshold only under the -1σ edge of the sensitivity band.

[1] G. Bertone, D. Hooper and J. Silk, Phys. Rep. **405**, 279 (2005).
[2] L. Roszkowski *et al.* Rep. Prog. Phys. **81**, 066201 (2018).
[3] T. Marrodán Undagoitia and L. Rauch, J. Phys. G **43**, no. 1, 013001 (2016)
[4] L. E. Strigari, Phys. Rep. **531**, 1 (2012).
[5] E. Aprile *et al.* (XENON Collaboration), Phys. Rev. Lett. **119**, 181301 (2017).
[6] D. S. Akerib *et al.* (LUX Collaboration), Phys. Rev. Lett. **118**, 021303 (2016).
[7] X. Cui *et al.* (PandaX-II Collaboration), Phys. Rev. Lett. **119**, 181302 (2017).
[8] E. Aprile *et al.* (XENON Collaboration), Eur. Phys. J. C **77**: 881 (2017).
[9] E. Aprile *et al.* (XENON Collaboration), Eur. Phys. J. C **75**: 546 (2015).
[10] P. Barrow *et al.* JINST **12**, no. 01, P01024 (2017).
[11] E. Aprile *et al.* (XENON Collaboration), JINST **9**, P11006 (2014).
[12] P. Sorensen, K. Kamdin. JINST **13**, P02032 (2018).
[13] D. Furse *et al.*. New J. Phys. **19** 053012 (2017)
[14] D. S. Akerib *et al.*, Phys. Rev. D **96**, 112009 (2017).
[15] E. Aprile *et al.* (XENON Collaboration), Phys. Rev. D **95**, 072008 (2017).
[16] R. F. Lang *et al.*, Nucl. Inst. and Meth. A **879**, 31 (2018).
[17] B. Riedel *et al.* PEARC '18, ISBN 978-1-4503-6446-1 (2018). doi:10.1145/3219104.3219155.
[18] XENON Collaboration. (2018). The pax data processor

v6.8.0. Zenodo. http://doi.org/10.5281/zenodo.1195785
[19] R. Saldanha *et al.*, Nucl. Inst. and Meth. A **863**, 35 (2017).
[20] C. H. Faham *et al.*, JINST **10**, P09010 (2015).
[21] D. S. Akerib *et al.* (LUX Collaboration), JINST **12**, P11022 (2017).
[22] J. Lewin and P. Smith, Astropart. Phys. **6** 87 (1996).
[23] E. Aprile *et al.* (XENON Collaboration), Eur. Phys. J. C **77**: 275 (2017).
[24] S. Lindemann, H. Simgen, Eur. Phys. J. C **74**, 2746 (2014).
[25] E. Aprile *et al.* (XENON Collaboration), Eur. Phys. J. C **78** :132 (2018).
[26] A. M. Serenelli *et al.*, Astro. Phys. Journal **743**, 29 (2011).
[27] D. Akimov *et al.* (COHERENT Collaboration), Science **357**, 1123-1126 (2017).
[28] S. Agostinelli *et al.*, Nucl. Inst. and Meth. A **506**, 250 (2003).
[29] E. Aprile *et al.* (XENON Collaboration), J. Cosmol. Astropart. Phys. **1604**, no. 04, 027 (2016)
[30] E. Aprile *et al.* (XENON Collaboration), Eur. Phys. J. C **77**: 890 (2017).
[31] W.B. Wilson *et al.*, LANL technical note LA-13639-MS (1999).
[32] R. Lemrani *et al.*, Nucl. Inst. and Meth. A **560**, 454 (2006).
[33] E. Aprile *et al.* (XENON Collaboration), Phys. Rev. D **97**, 092007 (2018).
[34] J. Thomas, and D. A. Imel, Phys. Rev. A **36**, 614 (1987).
[35] B. Lenardo *et al.* IEEE Trans. Nucl. Sci. **62**, 3387 (2015).
[36] D. S. Akerib et al. (LUX Collaboration), Phys. Rev. D **93**, 072009 (2016).
[37] E. M. Boulton *et al.*, JINST **12**, P08004 (2017).
[38] D. S. Akerib *et al.* (LUX Collaboration), Phys. Rev. D **96**, 112011 (2017).
[39] G. J. Feldman and R. D. Cousins, Phys. Rev. D **57**, 3873 (1998).
[40] C. Patrignani *et al.* (Particle Data Group), Chin. Phys. C **40**, 100001 (2016).
[41] F. James, Comput. Phys. Commun. **20**, 29 (1980).
[42] M. S. Bartlett, Biometrika **40** 3/4 (1953).
[43] N. Priel, L. Rauch, H. Landsman, A. Manfredini, and R. Budnik, J. Cosmol. Astropart. Phys. **5** 13 (2017).
[44] J. B. Albert *et al.* (EXO-200 Collaboration), Nature **510**, 225 (2014).